Published in final edited form as:
Neurotoxicology. 2009 November ; 30(6): 867–875. doi:10.1016/j.neuro.2009.07.007.

Altered Myelination and axonal integrity in Adults with Childhood Lead Exposure: A Diffusion Tensor Imaging Study

Christopher J. Brubaker[1,2], **Vincent J. Schmithorst**[2], **Erin N. Haynes**[3], **Kim N. Dietrich**[1,3], **John C. Egelhoff**[2], **Diana M. Lindquist**[2], **Bruce P. Lanphear**[1,4], and **Kim M. Cecil**[1,2]

[1] Cincinnati Children's Environmental Health Center at the Cincinnati Children's Hospital Medical Center, University of Cincinnati College of Medicine, Cincinnati, OH USA

[2] Department of Radiology, University of Cincinnati College of Medicine, Cincinnati, OH USA

[3] Department of Environmental Health, University of Cincinnati College of Medicine, Cincinnati, OH USA

[4] Child & Family Research Institute, BC Children's Hospital, Faculty of Health Sciences, Simon Fraser University, Vancouver, BC Canada

Abstract

Childhood lead exposure is associated with adverse cognitive, neurobehavioral and motor outcomes, suggesting altered brain structure and function. The purpose of this work was to assess the long-term impact of childhood lead exposure on white matter integrity in young adults. We hypothesized that childhood lead exposure would alter adult white matter architecture via deficits in axonal integrity and myelin organization. Adults (22.9 ± 1.5 years, range 20.0 to 26.1 years) from the Cincinnati Lead Study were recruited to undergo a study employing diffusion tensor imaging (DTI). The anatomic regions of association between water diffusion characteristics in white matter and mean childhood blood lead level were determined for ninety-one participants (52 female). Fractional anisotropy (FA), mean diffusivity (MD), axial diffusivity (AD), and radial diffusivity (RD) were measured on an exploratory voxel-wise basis. In adjusted analyses, mean childhood blood lead levels were associated with decreased FA throughout white matter. Regions of the corona radiata demonstrated highly significant lead-associated decreases in FA and AD and increases in MD and RD. The genu, body, and splenium of the corpus callosum demonstrated highly significant lead-associated decreases in RD, smaller and less significant decreases in MD, and small areas with increases in AD. The results of this analysis suggest multiple insults appear as distinct patterns of white matter diffusion abnormalities in the adult brain. Neurotoxic insults from the significant lead burden the participants experienced throughout childhood affect neural elements differently and may be related to the developmental stage of myelination at periods of exposure. This study indicates that childhood lead exposure is associated with a significant and persistent impact on white matter microstructure as quantified with diffusivity changes suggestive of altered myelination and axonal integrity.

Corresponding Author Address: Kim M. Cecil, PhD, Cincinnati Children's Hospital Medical Center, Department of Radiology/Imaging Research Center MLC 5033, 3333 Burnet Avenue, Cincinnati, OH 45229, United States of America, Phone: 513-636-8559, Fax: 513-636-3754, e-mail: kim.cecil@cchmc.org.

Keywords

myelination; internal capsule; corona radiata; corpus callosum

Introduction

Lead is a potent and pervasive environmental neurotoxicant that is especially harmful during childhood development. A diverse array of cognitive, neurobehavioral and motor problems are associated with childhood lead exposure, suggesting that lead causes widespread effects on brain development and functional outcomes. (Baghurst PA, 1995, Baghurst PA, 1992, Bellinger DC, 1992, Canfield RL, 2003, Dietrich KN, 1993, Dietrich KN, 1993, Ernhart CB, 1989, Ris MD, 2004, Surkan PJ, 2007). For persons who have blood lead levels exceeding 70μg/dL, which is often characterized by encephalopathy, conventional neuroimaging modalities such as computerized tomography (CT) and magnetic resonance imaging (MRI) can reveal macroscopic brain abnormalities. However, such examinations may fail to reveal brain abnormalities associated with lead exposure in persons with low to moderate blood lead levels (1–70μg/dL), independent of any cognitive and neurobehavioral manifestations. (Tuzun M, 2002, Mani J, 1998, Atre AL, 2006, al Khayat A, 1997

Only a few studies have sought to systematically examine the effects of lead on human brain structure and organization *in vivo*. In a series of volumetric analyses of organolead industrial workers exposed to lead primarily as adults, investigators found regions of gray matter volume loss associated with tibial lead levels (Stewart WF, 2006), and that areas of volume loss may be mediators of lead-associated cognitive changes (Schwartz BS, 2007). Studies of organolead workers have also linked white matter lesions to lead exposure (Bleecker ML, 2007, Stewart WF, 2006), and motor performance deficits (Bleecker ML, 2007). In a cohort of young adults exposed to lead during childhood, Cecil et al. observed a robust association between mean childhood blood lead levels and adult gray matter volume with loss in several brain regions, particularly the frontal cortex (Cecil KM, 2008). However, no white matter volume changes were found to be associated with mean childhood blood lead levels.

Experimental animal and *in vitro* exposure models reveal lead's toxicity to both neurons and glia through diverse mechanisms (Toscano CD and Guilarte TR, 2005, White LD, 2007). Lead may act as a calcium analog in neurons with exposure inhibiting glutamate release through binding to the NMDA receptor in an age-dependent and region specific manner (Guilarte TR, 1994), which would result in structural and functional differences despite uniform concentrations within the brain. Lead alters white matter via expression of genes essential to myelin formation (Deng W and Poretz RD, 2001, Zawia NH and Harry GJ, 1995), delayed myelin accumulation (Toews AD, 1983, Toews AD, 1980), delayed differentiation of oligodendrocyte progenitors (Deng W and Poretz RD, 2002,), disordered oligodrocyte architecture (Dabrowska-Bouta B, 1999), structural changes within the myelin sheath and disintegration of the multi-lamellar structure (Dabrowska-Bouta B, 2008) and astrogliosis (Selvin-Testa A, 1994, Struzynska L, 2001, Struzynska L, 2007). In exposing the immature rat brain to prolonged lead exposure, Struzynska demonstrated glial cell activation occurs with the elevation of GFAP and S-100βproteins, accompanied by increased cytokine production and evidence of axonal damage (Struzynska L, 2007). With such experimental evidence, we would expect damage to white matter in association with lead exposure in humans.

Diffusion tensor imaging (DTI), a recently developed MRI technique, affords sensitive microscopic evaluation of water diffusion properties within brain white matter. For several white matter diseases, such as multiple sclerosis, DTI can detect abnormalities in the diffusion properties of white matter within plaques as well as normal appearing white matter (NAWM).

We hypothesized that childhood lead exposure would result in altered adult white matter architecture via deficits in axonal integrity and myelin organization. We sought to reveal these deficits by investigating four quantitative diffusion parameters: fractional anisotropy (FA), mean diffusivity (MD), axial diffusivity (AD) and radial diffusivity (RD). FA, MD, AD and RD are derived from the three eigenvalues of the diffusion tensor model of water diffusion, representing diffusivities in a "voxel-wise" frame of reference (Basser PJ and Pierpaoli C, 1998, Pierpaoli C and Basser PJ, 1996). In other words, the smallest individual components of each image are quantified into these four parameters describing the behavior of water within the white matter and used for comparison analyses.

Normal cellular and tissue barriers, such as cell membranes and myelin sheaths, limit water diffusion within the white matter (Basser PJ and Pierpaoli C, 1996). Water diffusion occurs parallel to axonal fiber tracts as diffusion is restricted in the direction perpendicular to the fiber direction (Le Bihan D, 2001). This directional restriction is thought to arise from the tight, parallel packing of axonal fibers, and is considered to be a measure of white matter tissue organization (Le Bihan D, 2001). FA values reflect the degree of directional restriction of water diffusion with values ranging from 0 for isotropic (unrestricted, disorganized) to 1 for anisotropic (restricted, highly organized). A loss of directional coherence via *reduced* FA values indicates disorganization of white matter fibers. MD values measure the mean distance of water diffusion in all directions, which is restricted by white matter fibers, macromolecules and cell membranes. MD values express a measure of cellular integrity and structure with *increasing* MD values indicating loss of microstructure organization (Beaulieu C, 2002). Simply, the water can diffuse out more freely as barriers are damaged or destroyed. AD describes diffusion parallel to the fiber direction and yields information regarding axonal integrity and structure with *decreases* noted in animal models of optic nerve ischemia and multiple sclerosis (Kim JH, 2006, Kinoshita Y, 1999, Song S-K, 2003). RD describes diffusion perpendicular to the fiber direction, and informs about myelin sheath thickness and organization (Partridge SC, 2004, Song S-K, 2002, Song S-K, 2005, Suzuki Y, 2003). *Higher* RD values represent *less* myelination or diminished oligodendroglial integrity as more water diffusion occurs perpendicular to the axonal fiber tracts. The combination of FA, MD, AD, and RD analyses allows for sensitive, quantitative, noninvasive, *in-vivo* assessment of white matter architecture of an adult population with significant childhood lead exposure.

Methods

Participants

The Institutional Review Boards at the University of Cincinnati College of Medicine and the Cincinnati Children's Hospital Medical Center approved the study protocol. The participants in this study were recruited from the Cincinnati Lead Study (CLS), a longitudinal birth cohort study designed to evaluate the effects of low to moderate environmental lead exposure. The participants' mothers were enrolled to allow monitoring of blood lead levels for the participants prenatally, at birth, every three months to 60 months of age, and every 6 months from 60 to 78 months of age. Participants were stratified, based on their average lifetime lead exposure, into low, medium or high lead levels. Within each stratification level, participants were assigned a random number and participants with the lowest numbers were recruited first. At approximately 23 years of age, 100 participants from the original CLS cohort were recruited and provided informed consent for the study. Nine participants were excluded from final analyses due to obvious motion artifact (n = 2), grossly incorrect image segmentation (n = 4) or image registration errors (n = 3). The 91 participants (age = 22.9 ± 1.5 years, range = 20.0 to 26.1 years, 52 female) with useable imaging data had childhood mean blood lead levels of 12.9 ± 6.2 μg/dL (range = 4.8 to 37.3 μg/dL). The mean of twenty-three childhood blood lead assessments (3–78 months) for each participant was employed for comparison analyses, and

is referred to as MeanPb. The MeanPb concentrations have been previously reported as representative of childhood lead exposure within publications characterizing the CLS cohort (Dietrich KN, 1993, Dietrich KN, 1991). When no blood lead data was obtained for a given timepoint, missing values were imputed from a weighted average of a within-subject regression of blood lead on age and the cohort mean at each age. This imputation was performed to avoid excluding those participants who may have one or only a few missing blood lead measurements in the context of an otherwise data-rich exposure history. Analyses demonstrated that there were no significant differences in magnitude, direction or statistical significance of blood lead regression coefficients when comparing observed and imputed datasets with observed-only datasets. A summary of the study demographics and possible confounding variables is shown in Table 1.

Image Acquisition

Images were acquired on a 3T Trio MR imaging scanner (Siemens, Erlangen, Germany). A 46-section, diffusion-weighted, spin-echo echo-planar imaging scan sequence was acquired in the axial plane with the following parameters: TR/TE = 6000/87 ms; FOV = 25.6 × 25.6 cm; matrix = 128 × 128; section thickness = 2 mm; b-value = 1000 s/mm^2; and 4 repetitions. Diffusion-weighted scans were acquired in 12 optimized directions. Reference T2-weighted images (b = 0) were also acquired. The duration of the DTI sequence was 5 minutes and 48 seconds. In addition to the DTI sequence, a whole-brain three dimensional magnetization-prepared rapid acquisition of gradient echo (MPRAGE) high-resolution T1-weighted anatomic scan sequence was acquired with the following parameters: TR/TE = 2000/2.93 ms; FOV = 21.9 × 21.9 cm; matrix = 256 × 205; section thickness = 1 mm; number of averages = 1; and scan duration was 3 minutes and 50 seconds.

Data Processing

Image reconstruction, post-processing, and statistical analysis were performed using a combination of Statistical Parametric Mapping, version 5 (SPM5) (Wellcome Department of Cognitive Neurology, London) in Matlab 7.1 (The Mathworks, Inc., Natick, MA), our proprietary Cincinnati Children's Image Processing Software (CCHIPS) running in IDL (Research Systems, Boulder, CO) (Schmithorst VJ, 2008, Schmithorst VJ, 2005), and SAS 9.1 (SAS Institute, Cary, NC). Raw image reconstruction, calculation of parametric (FA, MD, AD and RD) values from diffusion tensors, and construction of individual white matter masks were performed in CCHIPS. SPM5 was used for subsequent bias correction, segmentation, spatial normalization, and co-registration of diffusion parametric (FA, MD, AD and RD) images to anatomic images. To reduce partial volume errors due to incorrect sampling of gray matter and 'bleeding' errors at the gray-white matter boundary, voxels included in final analyses had to meet two criteria: voxel-wise FA value > 0.25 and white matter probability > 0.9. CCHIPS was used to produce white matter masks from the normalized white matter images. These white matter masks were individually applied to diffusion parametric images exceeding a FA-threshold of greater than 0.25 to produce spatially normalized, individually masked diffusion parametric images used for statistical analysis.

Statistical Analyses

The associations between diffusion parametric data values and MeanPb were tested for statistical significance on a voxel-wise basis by multiple regression analysis using a general linear model (GLM).

To determine appropriate statistical thresholds corresponding to a voxel-wise corrected $p < 0.05$, CCHIPS was used to perform Monte Carlo simulations on the diffusion parametric data. The desired statistical thresholds were reached using a cluster size of 100 voxels, 3 mm post-

processing filter, and 2-tailed minimum Z thresholds of Z=5.6 for FA data, Z=5.0 for MD data, Z=5.4 for AD data, and Z=4.9 for RD data.

Confounding Variable Analyses

To determine potential confounding variables, we performed simple voxel-wise regressions between each diffusion parameter and MeanPb. The mean value of all the significantly associated voxels for a given parameter, noting single directions of association (positive or negative), was extracted for each participant and exported to SAS 9.1 (SAS Institute, Cary, NC). These mean values were used as outcome variables in the forward selection and backward elimination methods of variable selection in PROC REG. Continuous variables considered were age at imaging, birth weight, gestational age, maternal IQ, mean childhood HOME inventory, educational attainment, and Hollingshead socioeconomic status (SES) at imaging; categorical variables considered were sex, adult marijuana usage derived from a urine toxicology screening, maternal prenatal alcohol use, maternal prenatal cigarette use, and maternal prenatal marijuana use. Variables were included in the final regression model if any region achieved significance less than 0.1 (Pr > F) with either the forward selection or backward elimination method of variable selection.

Variables included in the final model for FA analysis were prenatal maternal alcohol use, prenatal maternal tobacco use, and maternal IQ; for MD analysis, prenatal maternal alcohol use, prenatal maternal tobacco use, and maternal IQ, and adult marijuana usage; for AD analysis, prenatal maternal marijuana use, adult marijuana usage, and age at imaging; for RD analysis, prenatal maternal alcohol use, gestational age, maternal IQ, and adult marijuana usage.

Using multiple regression analyses adjusted for significant confounding variables, we produced composite maps (Figure 1A–D) to demonstrate the statistically significant voxel-wise associations between MeanPb and each diffusion parameter, respectively. The minimum Z-statistic was chosen based upon Monte Carlo simulations and corresponds to a 2-tailed correct voxel-wise p value <0.05. Cool colors represent negative associations.

Results

The FA map demonstrated an inverse association between FA and MeanPb in diffusely scattered white matter regions, including the internal capsule, anterior and superior corona radiata (Figure 1A with inverse relationships are shown in blue).

The MD map exhibited both inverse and direct correlations with MeanPb; the primary inverse relationship observed in the corpus callosum, while the primary direct relationship noted in the superior corona radiata (Figure 1B with direct relationships shown in yellow and red).

The AD map revealed AD values within the anterior and superior corona radiata were inversely correlated with MeanPb, with a small focus of direct association found within the body of the corpus callosum (Figure 1C).

Finally, the RD map presents both inverse and direct correlations with MeanPb with the primary inverse relationship observed in the corpus callosum, and internal capsule, while the direct relationship noted in the superior corona radiata (Figure 1D).

Parametric values from smaller structures were also found significantly associated with MeanPb. These structures are listed within Table 2.

Discussion

Our study found that water diffusion metrics in the normal appearing white matter of participants from the CLS are associated with adjusted mean childhood blood lead levels. Our exploratory voxel by voxel analyses found for the primary DTI metric, FA, a reduction is demonstrated focally within the frontal, temporal, parietal and occipital lobes and to a general degree, bilaterally, throughout the cerebral hemispheres in association with increasing mean childhood blood lead levels. This metric suggests a general measure of disorganization within focal regions of the white matter with increasing exposure to lead. Subsequent probing with three other diffusion parameters, MD, AD and RD, suggest at least two significant patterns of insults may have occurred in association with childhood lead exposure.

Pattern within the Corona Radiata

The corona radiata are the white matter fibers linking the cerebral cortex to the internal capsule. The internal capsule connects the descending and ascending fibers to the thalamus, brainstem and spinal cord. Myelination within the corona radiata begins approximately at 34 weeks gestational age. However, completion of myelination and brain maturation varies with development across the corona radiata. Association (inferior fronto-occipital fasiculus (IFO), superior frontal-occipital fasciculus (SFO)), projection (anterior thalamic radiations (ATR), cortico-bulbar tract (CBT)), and limbic (stria terminalis (STR)) fibers found associated with the superior corona radiata demonstrated lead-associated decreases in FA and AD and increases in MD and RD. This DTI parametric pattern is the most typical reported in white matter disorders. The decline in FA and increase in MD are commonly interpreted as a loss of fiber directionality and increased water diffusion in all directions. Recently, mouse models of ischemia and multiple sclerosis suggest that AD and RD are fairly specific to axonal injury and myelin damage, respectively. (Song S-K, 2003) The decrease in AD may reflect some degree of axonal degeneration and/or astrogliosis. (Wang S, 2009) The increase in RD indicates atypical changes to the myelin have occurred in accordance with lead exposure. Combining these parameters, we find significant evidence that both the axonal and myelin constituents of white matter within the superior corona radiata are altered by lead exposure.

The corona radiata and its constituent fibers provide important connections between the frontal, parietal, temporal, and occipital lobes (Wakana S, 2004). These results are particularly interesting in light of prior studies showing evidence of lead-associated gray matter volume loss, particularly in the frontal lobes (Cecil KM, 2008). The inferior fronto-occipital fasciculus is an association bundle connecting the frontal with the parietal and occipital lobes, and these findings suggest changes in axonal integrity that might parallel loss of cortical gray matter. Lead-associated fine motor changes have been observed in the CLS cohort (Dietrich KN, 1993, Dietrich KN, 1987, Ris MD, 2004), and changes in axonal integrity in the corticobulbar tract or thalamic radiations could all contribute to motor problems. Another complementary interpretation for these findings is that the long association fibers retained more connections during developmental pruning, resulting in regions with an overabundance of narrow, thinly myelinated axons. Such axons would not function optimally. Thus, the observed diffusion changes could be due to increased fiber density concurrent with loss of myelin layers and/or myelin organization. Finally, white matter in this region could have undergone mild gliosis secondary to tissue damage, which would also be expected alter diffusion.

Pattern within the Corpus Callosum and Superior Longitudinal Fasciculus

The corpus callosum is the largest white matter structure in the brain, with approximately 200–250 million contralateral axonal projections providing communication between the two hemispheres. It develops in the first trimester, with myelination completed in the first year of life. We did not observe an association between FA and adjusted MeanPb in corpus callosum,

however, there were striking inverse associations between RD and adjusted MeanPb in the genu, body and splenium of the corpus callosum suggesting an abnormality of the myelin. The MD map exhibited an inverse relationship in the splenium alone. The AD map revealed a small focus of direct association found within the body of the corpus callosum.

The superior longitudinal fasciculus (SLF) is a complicated fiber tract connecting many brain regions, including the frontal lobes to the parieto-temporal association areas, which have been implicated in proprioceptive coding, visuospatial attention and performance, language, and auditory perception (Makris N, 2005). Similar to the corpus callosum, we found significant inverse associations between adjusted mean childhood blood lead levels and MD and RD, but no significant associations were found with AD in this region. Unlike the corpus callosum, an inverse relationship was found between FA and MeanPb within this region.

Decreases in RD values have been observed in association with axonal myelination in human studies of white matter maturation (Partridge SC, 2004, Suzuki Y, 2003) and remyelination after *in vitro* models of demyelination (Song S-K, 2005). The striking inverse association observed between RD and adjusted mean childhood blood lead levels in the genu, body, and splenium of the corpus callosum, and to a lesser extent in the SLF, suggests *increased* myelination in these regions associated with childhood lead exposure in the absence of frank axonal changes (Song S-K, 2003, Song S-K, 2002). The significance of these findings is uncertain, however, complementary to the findings of a functional MRI study obtained from a smaller cohort of the Cincinnati Lead Study while employing a verb generation paradigm (Yuan W, 2006). Yuan and colleagues demonstrated that increased utilization of the contralateral homologues of Wernicke's and Broca's areas were associated with mean childhood blood lead levels. The corpus callosum provides the major inter-hemispheric connection of the brain. Increased myelination of the corpus callosum and SLF could indicate increased connectivity between these regions, possibly as compensation for reduced left lateralized brain activation associated with lead exposure.

Pattern within the Internal Capsule

As mentioned previously, the internal capsule connects the descending and ascending fibers to the thalamus, brainstem and spinal cord. Myelination of the posterior limb of the internal capsule begins around 32 weeks gestational age and is essentially is completed by 44 weeks. However, the anterior limb lags behind with myelination beginning in the eighth month of gestation. We observed an inverse relationship between FA and adjusted MeanPb in the posterior limb of the internal capsule (Figure 1, levels −3 to +13). The MD map exhibited an inverse relationship between MD and adjusted MeanPb only in the bend of the internal capsule, known as the genu, which involves the corticobulbar tract. The AD map revealed no association between AD and adjusted MeanPb. Striking inverse associations between RD and adjusted MeanPb in the genu, anterior and posterior limbs of the internal capsule (Figure 4, levels (Figure 4, levels −3 to +17) suggests an abnormality of the myelin. The pattern is similar to that of the corpus callosum, with the additional finding of significant FA association.

Myelination and Pattern Involvement

Our findings indicate that brain myelination is altered by childhood lead exposure. Reduced FA and AD with increased MD and RD in association with MeanPb are consistent with both axonal and myelin injury within the corona radiata. This pattern of DTI parameters has been validated in numerous imaging studies of disorders with pathological evidence of white matter injury. The corona radiata is a later myelinating structure requiring prolonged maturation of cortical connections. The fetal and developmental lead exposure for this later-developing structure produces adverse effects to both axonal and myelin units. In contrast, the corpus callosum and internal capsule show evidence of altered, and perhaps increased myelination

without significant axonal involvement. The corpus callosum and internal capsule, particularly the posterior limb, are structures whose myelination begins in utero and is usually completed within the first year of post-natal life. The relative early completion of myelination may afford axonal protection and some measure of adaptation for these structures in response to elevated lead exposures.

It is important to distinguish the results of this DTI study from one that compares findings in persons with a symptomatic white matter disorder to those of healthy controls. As there are no "unleaded" individuals, especially those who are as well characterized demographically and quantitatively for lead exposure as the CLS, we cannot study a relevant comparison group. Instead, our approach uses regression analyses to demonstrate the parametric changes associated with mean childhood blood lead levels as it increases from approximately 5 to 37 μg/dL, with a majority between 5 and 20 μg/dL in the CLS population. The CLS population does not present with typical clinical or imaging features of white matter disorders, however, the cognitive, behavior and motor characteristics of this population may represent a sub-clinical disorder. The absence of macroscopic imaging findings does not preclude microscopic brain abnormalities as recognized in many developmental, behavioral and psychiatric conditions. Thus, the findings of this work may offer neurobiological insights to the recognized adverse neuropsychological outcomes associated with childhood lead exposure.

Limitations

Maternal and individual factors (i.e., IQ) and exposures to substances such as marijuana are likely to influence white matter structure and organization. However, our analyses found that the associations of all four diffusion metrics were significantly greater for mean childhood blood lead levels than that of the other co-exposure variables. In preparing an appropriate model, we utilized a novel method of covariate selection for this study. In prior studies employing fMRI (Yuan W, 2006) and volumetric analyses (Cecil KM, 2008), the significance of potential confounding variables was assessed by measuring the change in beta for the covariate of interest in a separate, bivariate model for each potential confounding variable. While conceptually simple, this approach was cumbersome and allowed limited diagnostic capability. In this study, the more established regression diagnostic tools available under PROC REG in SAS (SAS Institute, Inc, Cary, NC) were adapted to our diffusion based parametric outcome measures. Compared with previous methods of covariate selection, the method employed in this study was less time consuming, directly related to established biostatistical and epidemiological methods and offered a greater selection of diagnostic assays. However, it required a significant distillation of data because one mean diffusion parameter value is generated per region per participant. While this represents an acceptable compromise, particularly when coupled with our selection of conservative Z thresholds and inclusive implementation of the forward selection and backward elimination methods of variable selection, it would be preferable to assess the influence of potential confounders in a voxel by voxel manner. We are unaware of any readily accessible software package that allows this type of analysis.

Individual anatomic differences found even in normalized images result in blending of diffusion values from different structures or unmasked space, reducing specificity and statistical power in confounder selection and regression analyses. These partial volume errors are particularly problematic for small, specific anatomic locations such as the internal capsule and areas where gray and white matter interface such as in the anterior and posterior regions of this analysis. Statistical power is thus not uniform across white matter, but is limited in some areas by underlying white matter anatomic variability. Similarly, interpretation of voxel-wise diffusivity findings in the anterior and posterior regions is particularly complicated by underlying anatomic heterogeneity between participants, limiting the sensitivity of voxel-wise

comparisons in these highly anatomically heterogeneous areas (Ashburner J and Friston KJ, 2000).

Conclusions

This study investigated the effects of environmental lead exposure on white matter by diffusion tensor metrics. Analyses of four quantitative diffusion parameters provided a detailed quantitative assessment of the effects of childhood lead exposure on white matter. The imaging data supports evidence from clinical and experimental investigations that lead affects white matter structure via deficits in axonal integrity and myelin organization. Such alterations likely depend on multiple factors, which include lead concentrations particularly the levels within the brain, the exposure duration and timing during brain development and maturation. Further studies could examine how these factors modulate changes in imaging metrics and ultimately, clinical outcome.

Acknowledgments

The authors acknowledge the efforts of Stephanie D. Wessel, MS, Kendall J. O'Brien, BS, RT, and R. Scott Dunn, RT for providing imaging technical support. We are also grateful to members of the Cincinnati Lead Study Cohort and their families for their participation in this research.

This work was supported by grants from the National Institutes of Health, NIEHS P01 ES011261, NIEHS R01 ES015559, NIEHS R21 ES013524, NCI R01 CA112182, M01 RR08084 from the General Clinical Research Centers Program, and the Environmental Protection Agency R82938901.

References

al Khayat A, Menon NS, Alidina MR. Acute lead encephalopathy in early infancy--clinical presentation and outcome. Ann Trop Paediatr 1997 Mar;17:39–44. [PubMed: 9176576]

Ashburner J, Friston KJ. Voxel-based morphometry--the methods. Neuroimage 2000 Jun;11:805–21. [PubMed: 10860804]

Atre AL, Shinde PR, Shinde SN, Wadia RS, Nanivadekar AA, Vaid SJ, Shinde RS. Pre- and posttreatment MR imaging findings in lead encephalopathy. Am J Neurorad 2006 Apr;27:902–3.

Baghurst PA, McMichael AJ, Tong S, Wigg NR, Vimpani GV, Robertson EF. Exposure to environmental lead and visual-motor integration at age 7 years: The port pirie cohort study. Epidemiology 1995 Mar; 6:104–9. [PubMed: 7742393]

Baghurst PA, McMichael AJ, Wigg NR, Vimpani GV, Robertson EF, Roberts RJ, et al. Environmental exposure to lead and children's intelligence at the age of seven years. The port pirie cohort study. N Engl J Med 1992 Oct 29;327:1279–84. [PubMed: 1383818]

Basser PJ, Pierpaoli C. Microstructural and physiological features of tissues elucidated by quantitative-diffusion-tensor mri. J Magn Reson B 1996 Jun;111:209–19. [PubMed: 8661285]

Basser PJ, Pierpaoli C. A simplified method to measure the diffusion tensor from seven mr images. Magn Reson Med 1998 Jun;39:928–34. [PubMed: 9621916]

Beaulieu C. The basis of anisotropic water diffusion in the nervous system - a technical review. NMR Biomed 2002 Nov-Dec;15:435–55. [PubMed: 12489094]

Bellinger DC, Stiles KM, Needleman HL. Low-level lead exposure, intelligence and academic achievement: A long-term follow-up study. Pediatrics 1992 Dec;90:855–61. [PubMed: 1437425]

Bleecker ML, Ford DP, Vaughan CG, Walsh KS, Lindgren KN. The association of lead exposure and motor performance mediated by cerebral white matter change. Neurotoxicology 2007 Mar;28:318–23. [PubMed: 16781776]

Canfield RL, Henderson CR Jr, Cory-Slechta DA, Cox C, Jusko TA, Lanphear BP. Intellectual impairment in children with blood lead concentrations below 10 microg per deciliter. N Engl J Med 2003 Apr 17;348:1517–26. [PubMed: 12700371]

Cecil KM, Brubaker CJ, Adler CM, Dietrich KN, Altaye M, Egelhoff JC, et al. Decreased brain volume in adults with childhood lead exposure. PLoS Med 2008 May 27;5:e112. [PubMed: 18507499]

Dabrowska-Bouta B, Struzynska L, Walski M, Rafalowska U. Myelin glycoproteins targeted by lead in the rodent model of prolonged exposure. Food Chem Toxicol 2008 Mar;46:961–6. [PubMed: 18077072]

Dabrowska-Bouta B, Sulkowski G, Bartosz G, Walski M, Rafalowska U. Chronic lead intoxication affects the myelin membrane status in the central nervous system of adult rats. J Mol Neurosci 1999 Aug-Oct;13:127–39. [PubMed: 10691300]

Deng W, Poretz RD. Lead exposure affects levels of galactolipid metabolic enzymes in the developing rat brain. Toxicol Appl Pharmacol 2001 Apr 15;172:98–107. [PubMed: 11298496]

Deng W, Poretz RD. Protein kinase c activation is required for the lead-induced inhibition of proliferation and differentiation of cultured oligodendroglial progenitor cells. Brain Res 2002 Mar 1;929:87–95. [PubMed: 11852034]

Dietrich KN, Berger OG, Succop PA. Lead exposure and the motor developmental status of urban six-year-old children in the cincinnati prospective study. Pediatrics 1993 Feb;91:301–7. [PubMed: 7678702]

Dietrich KN, Berger OG, Succop PA, Hammond PB, Bornschein RL. The developmental consequences of low to moderate prenatal and postnatal lead exposure: Intellectual attainment in the cincinnati lead study cohort following school entry. Neurotoxicol Teratol 1993 Jan-Feb;15:37–44. [PubMed: 8459787]

Dietrich KN, Krafft KM, Bornschein RL, Hammond PB, Berger O, Succop PA, et al. Low-level fetal lead exposure effect on neurobehavioral development in early infancy. Pediatrics 1987 Nov;80:721–30. [PubMed: 2444921]

Dietrich KN, Succop PA, Berger OG, Hammond PB, Bornschein RL. Lead exposure and the cognitive development of urban preschool children: The cincinnati lead study cohort at age 4 years. Neurotoxicol Teratol 1991 Mar-Apr;13:203–11. [PubMed: 1710765]

Ernhart CB, Morrow-Tlucak M, Wolf AW, Super D, Drotar D. Low level lead exposure in the prenatal and early preschool periods: Intelligence prior to school entry. Neurotoxicol Teratol 1989 Mar-Apr; 11:161–70. [PubMed: 2733654]

Guilarte TR, Miceli RC, Jett DA. Neurochemical aspects of hippocampal and cortical pb2+ neurotoxicity. Neurotoxicology 1994 Fall;15:459–66. [PubMed: 7854579]

Kim JH, Budde MD, Liang HF, Klein RS, Russell JH, Cross AH, et al. Detecting axon damage in spinal cord from a mouse model of multiple sclerosis. Neurobiol Dis 2006 Mar;21:626–32. [PubMed: 16298135]

Kinoshita Y, Ohnishi A, Kohshi K, Yokota A. Apparent diffusion coefficient on rat brain and nerves intoxicated with methylmercury. Environ Res 1999 May;80:348–54. [PubMed: 10330308]

Le Bihan D, Mangin JF, Poupon C, Clark CA, Pappata S, Molko N, et al. Diffusion tensor imaging: Concepts and applications. J Magn Reson Imaging 2001 Apr;13:534–46. [PubMed: 11276097]

Makris N, Kennedy DN, McInerney S, Sorensen AG, Wang R, Caviness VS Jr, et al. Segmentation of subcomponents within the superior longitudinal fascicle in humans: A quantitative, in vivo, dt-mri study. Cereb Cortex 2005 Jun;15:854–69. [PubMed: 15590909]

Mani J, Chaudhary N, Kanjalkar M, Shah PU. Cerebellar ataxia due to lead encephalopathy in an adult. J Neurol Neurosurg Psychiatry 1998 Nov;65:797. [PubMed: 9810963]

Partridge SC, Mukherjee P, Henry RG, Miller SP, Berman JI, Jin H, et al. Diffusion tensor imaging: Serial quantitation of white matter tract maturity in premature newborns. Neuroimage 2004 Jul; 22:1302–14. [PubMed: 15219602]

Pierpaoli C, Basser PJ. Toward a quantitative assessment of diffusion anisotropy. Magn Reson Med 1996 Dec;36:893–906. [PubMed: 8946355]

Ris MD, Dietrich KN, Succop PA, Berger OG, Bornschein RL. Early exposure to lead and neuropsychological outcome in adolescence. J Int Neuropsychol Soc 2004 Mar;10:261–70. [PubMed: 15012846]

Schmithorst VJ, Holland SK, Dardzinski BJ. Developmental differences in white matter architecture between boys and girls. Hum Brain Mapp 2008 Jun;29:696–710. [PubMed: 17598163]

Schmithorst VJ, Wilke M, Dardzinski BJ, Holland SK. Cognitive functions correlate with white matter architecture in a normal pediatric population: A diffusion tensor mri study. Hum Brain Mapp 2005 Oct;26:139–47. [PubMed: 15858815]

Schwartz BS, Chen S, Caffo B, Stewart WF, Bolla KI, Yousem D, et al. Relations of brain volumes with cognitive function in males 45 years and older with past lead exposure. Neuroimage 2007 Aug 15;37:633–41. [PubMed: 17600728]

Selvin-Testa A, Loidl CF, Lopez-Costa JJ, Lopez EM, Pecci-Saavedra J. Chronic lead exposure induces astrogliosis in hippocampus and cerebellum. Neurotoxicology 1994 Summer;15:389–401. [PubMed: 7991228]

Song S-K, Sun S-W, Ju W-K, Lin S-J, Cross AH, Neufeld AH. Diffusion tensor imaging detects and differentiates axon and myelin degeneration in mouse optic nerve after retinal ischemia. NeuroImage 2003;20:1714–22. [PubMed: 14642481]

Song S-K, Sun S-W, Ramsbottom MJ, Chang C, Russell J, Cross AH. Dysmyelination revealed through mri as increased radial (but unchanged axial) diffusion of water. NeuroImage 2002;17:1429–36. [PubMed: 12414282]

Song S-K, Yoshino J, Le TQ, Lin S-J, Sun S-W, Cross AH, et al. Demyelination increases radial diffusivity in corpus callosum of mouse brain. NeuroImage 2005;26:132–40. [PubMed: 15862213]

Stewart WF, Schwartz BS, Davatzikos C, Shen D, Liu D, Wu X, et al. Past adult lead exposure is linked to neurodegeneration measured by brain mri. Neurology 2006 May 23;66:1476–84. [PubMed: 16717205]

Struzynska L, Bubko I, Walski M, Rafalowska U. Astroglial reaction during the early phase of acute lead toxicity in the adult rat brain. Toxicology 2001 Aug 28;165:121–31. [PubMed: 11522370]

Struzynska L, Dabrowska-Bouta B, Koza K, Sulkowski G. Inflammation-like glial response in lead-exposed immature rat brain. Toxicol Sci 2007 Jan;95:156–62. [PubMed: 17047031]

Surkan PJ, Zhang A, Trachtenberg F, Daniel DB, McKinlay S, Bellinger DC. Neuropsychological function in children with blood lead levels <10 microg/dl. Neurotoxicology 2007 Nov;28:1170–7. [PubMed: 17868887]

Suzuki Y, Matsuzawa H, Kwee IL, Nakada T. Absolute eigenvalue diffusion tensor analysis for human brain maturation. NMR Biomed 2003 Aug;16:257–60. [PubMed: 14648885]

Toews AD, Blaker WD, Thomas DJ, Gaynor JJ, Krigman MR, Mushak P, et al. Myelin deficits produced by early postnatal exposure to inorganic lead or triethyltin are persistent. J Neurochem 1983 Sep; 41:816–22. [PubMed: 6875567]

Toews AD, Krigman MR, Thomas DJ, Morell P. Effect of inorganic lead exposure on myelination in the rat. Neurochem Res 1980 Jun;5:605–16. [PubMed: 7402432]

Toscano CD, Guilarte TR. Lead neurotoxicity: From exposure to molecular effects. Brain Res Brain Res Rev 2005 Nov;49:529–54. [PubMed: 16269318]

Tuzun M, Tuzun D, Salan A, Hekimoglu B. Lead encephalopathy: CT and MR findings. J Comput Asst Tomogr 2002 May-Jun;26:479–81.

Wakana S, Jiang H, Nagae-Poetscher LM, van Zijl PC, Mori S. Fiber tract-based atlas of human white matter anatomy. Radiology 2004 Jan;230:77–87. [PubMed: 14645885]

Wang S, Wu EX, Qiu D, Leung LH, Lau HF, Khong PL. Longitudinal diffusion tensor magnetic resonance imaging study of radiation-induced white matter damage in a rat model. Cancer research 2009 Feb 1;69:1190–8. [PubMed: 19155304]

White LD, Cory-Slechta DA, Gilbert ME, Tiffany-Castiglioni E, Zawia NH, Virgolini M, et al. New and evolving concepts in the neurotoxicology of lead. Toxicol Appl Pharmacol 2007 Nov 15;225:1–27. [PubMed: 17904601]

Yuan W, Holland SK, Cecil KM, Dietrich KN, Wessel SD, Altaye M, et al. The impact of early childhood lead exposure on brain organization: A functional magnetic resonance imaging study of language function. Pediatrics 2006 Sep;118:971–7. [PubMed: 16950987]

Yuan W, Szaflarski JP, Schmithorst VJ, Schapiro M, Byars AW, Strawsburg RH, et al. Fmri shows atypical language lateralization in pediatric epilepsy patients. Epilepsia 2006 Mar;47:593–600. [PubMed: 16529628]

Zawia NH, Harry GJ. Exposure to lead-acetate modulates the developmental expression of myelin genes in the rat frontal lobe. Int J Dev Neurosci 1995 Oct;13:639–44. [PubMed: 8553899]

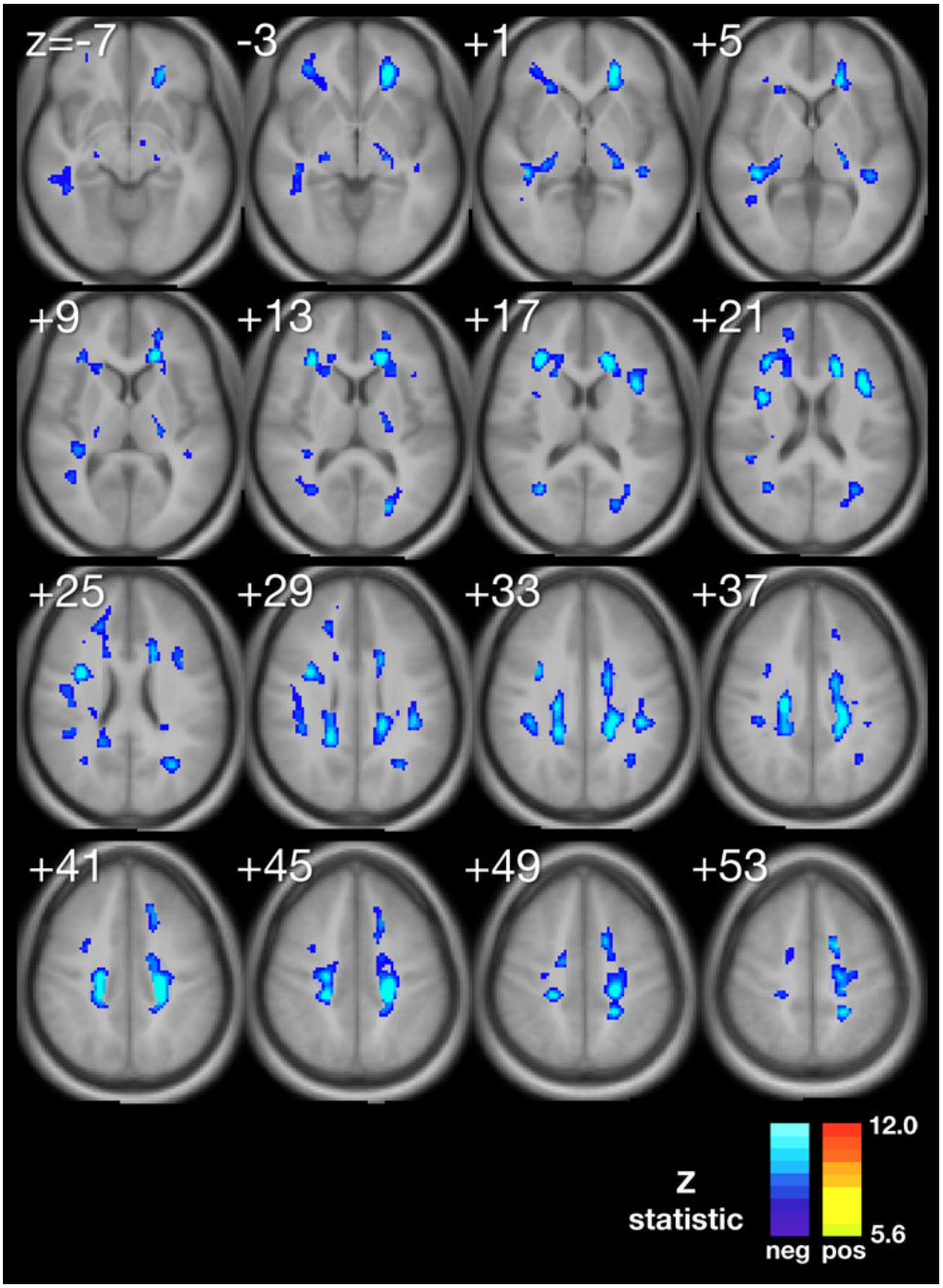

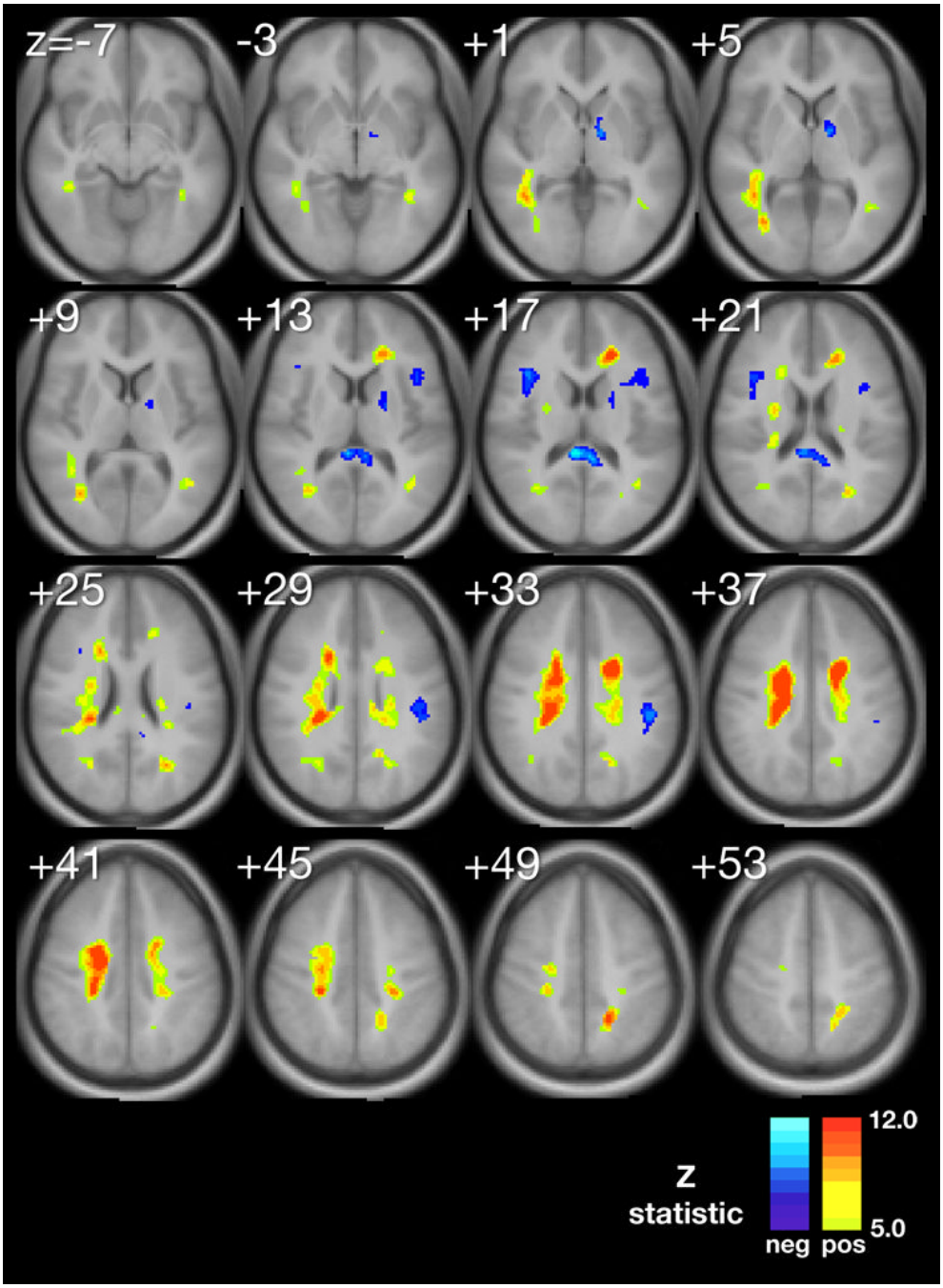

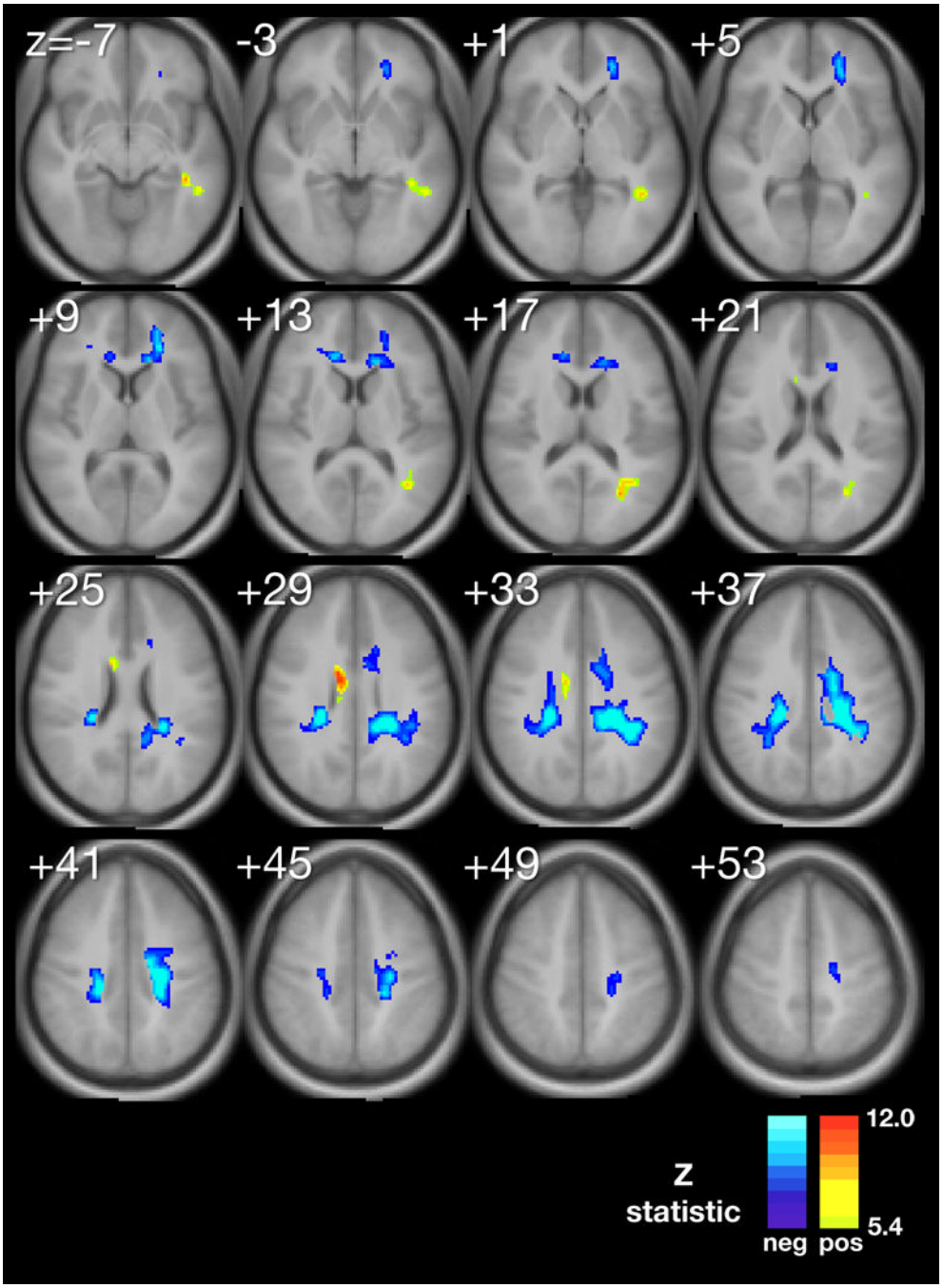

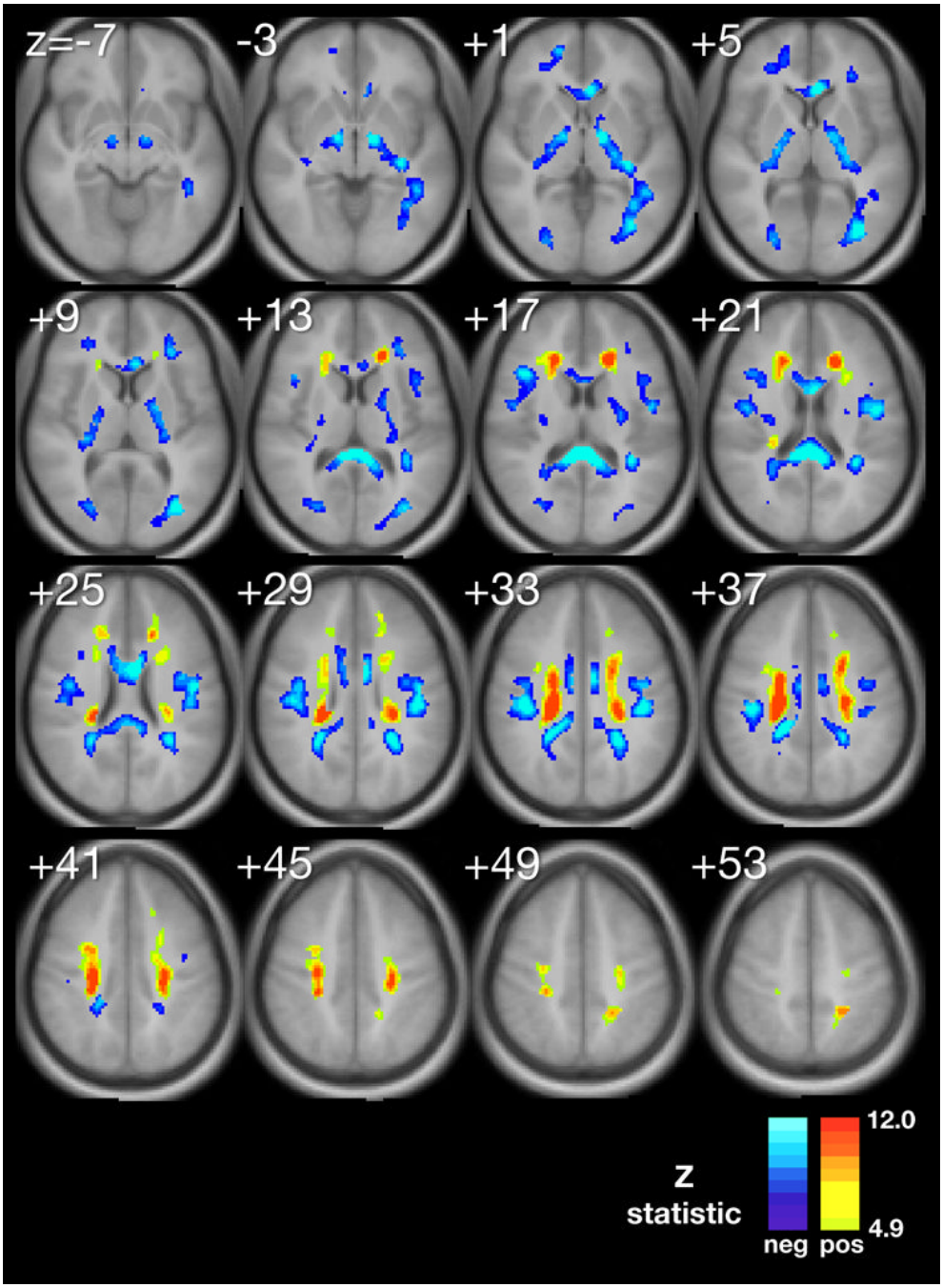

Figure 1.

A–D. Composite maps demonstrating regions of significant voxel-wise association between mean childhood blood lead and *A*, fractional anisotropy, *B*, mean diffusivity, *C*, axial difffusivity and *D*, radial diffusivity, adjusted for significant confounders, respectively. The minimum Z statistic was chosen based on Monte Carlo simulations and corresponds to a 2-tailed, corrected voxel-wise p value < 0.05. Cold colors represent negative associations.

Table 1

Characteristics of Participants and their Mothers

Mean Childhood Blood Lead (μg/dL)	12.9 ± 6.2 (4.8 – 37.2)
Age at imaging (years)	22.9 ± 1.5 (20.0 – 26.1)
Full-scale IQ	88.3 ± 11.4 (50 – 114)
Birth Weight (g)	3100 + 455 (1990 – 4340)
Gestational Age (weeks)	39.3 ± 1.7 (35 – 43)
Hollingshead SES at imaging	21.3 ± 7.8 (11 – 47)
Mean childhood HOME score	32.0 ± 4.2 (17 – 43)
Educational attainment (years in school)	11.7 ± 1.5 (8 – 16)
Maternal IQ	75.7 ± 9.3 (55 – 100)
Marijuana use at time of imaging*	36 positive (40%)
Prenatal Maternal Cigarette Use	39 positive (41%)
Prenatal Maternal Alcohol Use	15 positive (16%)
Prenatal Maternal Marijuana Use	13 positive (14%)
Prenatal Maternal Narcotic Use	1 positive (1%)

The demographics for the 91 participants include all variables considered as potential confounders in multiple regression analyses. Values are given as mean ± SD (minimum value – maximum value).

*Results based upon urine toxicology drugs of abuse screening collected at time of imaging.

Table 2

White Matter Tracts with Significant Lead-Associated Diffusion Changes

Anterior thalamic radiations (ATR)
Cingulum (CG)
Corona radiata (CR)
Corticobulbar tract (CBT)
Inferior longitudinal fasciculus (ILF)
Superior longitudinal fasciculus (SLF)
Inferior fronto-occipital fasciculus (IFO)
Superior fronto-occipital fasciculus (SFO)
Stria terminalis (STR)
Uncinate fasciculus (UNC)
Anterior callosal fibers (forceps minor)
Posterior callosal fibers (forceps major)
Genu of corpus callosum (GCC)
Body of corpus callosum (BCC)
Splenium of corpus callosum (SCC)
Tapetum (TPT) [passes through SCC]
Anterior limb of internal capsule (ALIC)
Genu of internal capsule (GIC)
Posterior limb of internal capsule (PLIC)